

# A general social contagions dynamics on interdependent lattices

**Panpan Shu<sup>1</sup>, Wei Wang<sup>2</sup>, Lidia A. Braunstein<sup>3,4</sup>**

<sup>1</sup> School of Sciences, Xi'an University of Technology, Xi'an 710054, China

<sup>2</sup> College of Computer Science and Technology, Chongqing University of Posts and Telecommunications, Chongqing 400065, China

<sup>3</sup> Instituto de Investigaciones Físicas de Mar del Plata (IFIMAR)-Departamento de Física, Facultad de Ciencias Exactas y Naturales, Universidad Nacional de Mar del Plata-CONICET - Funes 3350, (7600) Mar del Plata, Argentina

<sup>4</sup> Center for Polymer Studies and Department of Physics, Boston University - Boston, Massachusetts 02215, USA

E-mail: wwzqbx@hotmail.com

**Abstract.** The dynamical processes on interdependent spatial networks have attracted increasing interest in recent years, but the studies related to the complex contagions are relatively lack. Based on a general social contagions model, we numerically study how the interdependent spatial systems composed of two interdependent planar lattices influence the dynamics of social contagions. Once the rate of information transmission or the probability of behavior adoption is settled, the strong interdependent lattices could easily stimulate the contagion process and improve the final density of adopted individuals significantly. We perform finite-size analysis and confirm that the phase transition of prevalence with transmission rate is second-order, but even for the relatively small transmission rate, the phase transition of prevalence versus the adoption probability is first-order. Although the large transmission rate or the large adoption probability could promote the final adopted density in the weak interdependent lattices, phase transition of prevalence remains second-order. These findings provide us with a deep understanding of the social contagion dynamics in interdependent lattices.

*Keywords:* social contagions, interdependent lattices, phase transition

**Contents**

**1 Introduction 2**

**2 Model 3**

2.1 Interdependent spatial network . . . . . 3

2.2 Dynamics of spatial social contagion . . . . . 3

**3 Results 5**

**4 Conclusions 8**

**1. Introduction**

Many real-world networks are often interdependent and exhibit spatial structures [1, 2, 3, 4]. As a typical example, the nodes in a communications network strongly depend on the nodes in the power grid network for electricity while the power stations depend on the communication nodes for control, where both networks are embedded in the two-dimensional space [2]. Previous studies have revealed that the interdependent spatial networks can significantly influence the dynamical processes in them [3, 4, 5, 6, 7, 8, 9]. For example, reducing the spatial distance between the interdependent nodes can cause different types of phase transition in the percolation process [10], and the system can collapse in an abrupt transition when the fraction of dependency links increases to a certain value [11]. The propagation of cascading overloads is characterized by a finite linear propagation velocity on spatially embedded networks [12]. In particular, a localized attack can cause substantially more damage to spatially embedded systems with dependencies than an equivalent random attack [13]. Spatial networks are typically described by lattices [14, 15]. The related studies have found that asymmetric coupling between interdependent lattices can greatly promote collective cooperation [16], and the epidemic threshold in interconnected lattices decreases as the spatial length of interconnected links increases [17].

Unlike the epidemic dynamics, the dynamics of social contagions [18, 19, 20, 21, 22, 23] range from the adoption of social innovations [24, 25, 26, 27, 28] to the prevalence of healthy behaviors [29]. The related studies showed that multiple affirmations of the credibility and legitimacy of a piece of news or a new trend are ubiquitous in social contagions. The individual’s probability of adopting a new social behavior depends upon the accumulative total number of effective contacts within neighbors, which is described by the social reinforcement effect [29, 31, 32, 33, 34, 35]. Assuming that a susceptible individual will adopt the social behavior once the number or fraction of its adopted neighbors exceeds an adoption threshold, the threshold model has been widely used to describe the social reinforcement effect [36]. Using the threshold model, network characteristics related to social contagions such as the clustering coefficient [37], community structure [38, 39], and multiplexity [40, 41, 42, 43] have been explored, but less study was focused on the social contagions in interdependent spatial networks. Moreover, the social enforcement effect in traditional threshold model

usually enables multiple passes on the information between an adopted individual and its susceptible neighbors. In some social contagion processes, such as the spread of high-risk social movements, avant garde fashions, and unproven technologies [34], redundant transmission of related information between two individuals is unnecessary because a susceptible individual can guarantee the credibility and legitimacy of the behavior only to some extent [29]. Wang *et al.* investigated the non-redundant threshold model in random networks and found the crossover in phase transition [19], but the systematic study on this aspect is still rare, especially scarce in interdependent spatial networks.

In this work we study the non-redundant social contagions on interdependent lattice networks using a novel spatial social contagion model. We show numerically how the individuals' memory and dependency infection influence the prevalence of social contagions in interdependent lattice networks. More importantly, we find out the important roles of individuals' memory and dependency infection in the phase transitions. The paper is organized as follows. In Sec. 2, we describe the interdependent spatial network and the social dynamical process on it. In Sec. 3, we investigate the prevalence and the type of phase transition using finite-size analyses. Finally, we draw conclusions in Sec. 4.

## 2. Model

### 2.1. Interdependent spatial network

The interdependent spatial network is made up of two identical planar lattices  $A$  and  $B$  of linear size  $L$  and  $N = L \times L$  nodes with periodic boundaries. In each lattice all nodes are arranged in a matrix of  $L \times L$ , and each node is connected to its four neighbors in the same lattice via connectivity links (i.e., links between two nodes in the same lattice). The  $p$  fraction of nodes in lattice  $A$  are randomly selected as dependency nodes. Each dependency node  $A_i$  in lattice  $A$  will be connected to one and only one node  $B_j$  randomly selected in lattice  $B$  via a dependency link (i.e., the link between a nodes in lattice  $A$  and a node in lattice  $B$ ). Thus, each dependency node has only one dependency link. The total number of dependency links in the interdependent spatial network is determined by the parameter  $p$ . Obviously, the more the dependency links are, the more interdependent the two lattices become. For simplicity, the networks with a large  $p$  value are defined as the strong interdependent networks, and those with a small  $p$  value are defined as the weak ones.

### 2.2. Dynamics of spatial social contagion

The population in the interdependent spatial networks are grouped into susceptible (S), adopted (A) and recovered (R) compartments. The susceptible individuals have not adopted the behavior and are susceptible to the behavior information. The adopted individuals have adopted the behavior and are able to transmit the information to its susceptible neighbors. The recovered individuals become immune to the behavior and are no longer involved. Within the same lattice, individuals can retain their memory of previous behavior information received from neighbors. A susceptible individual adopts the new behavior with a specified probability

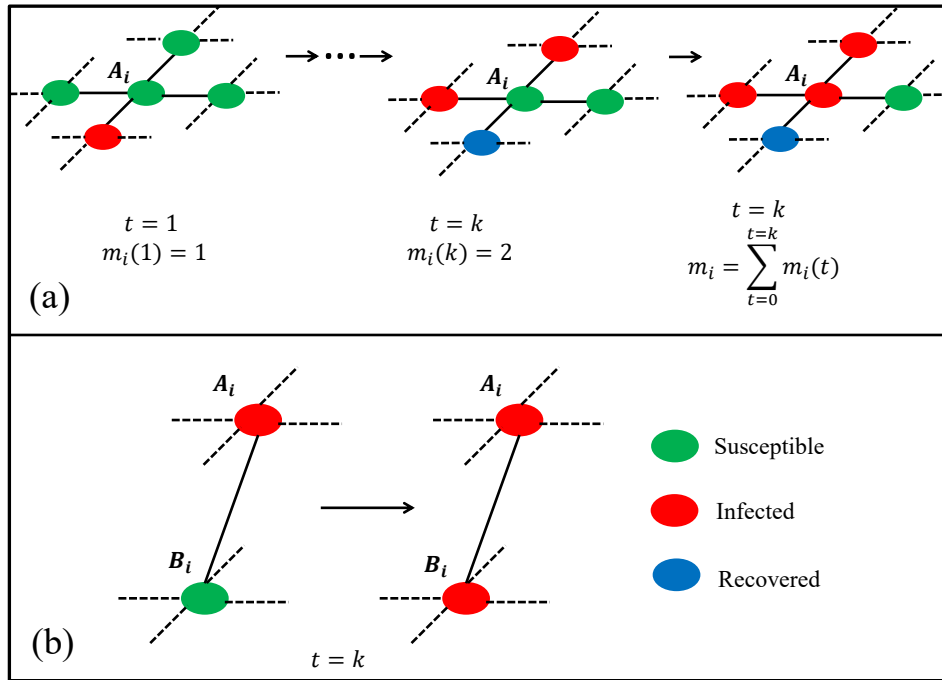


**Figure 1.** (Color online) **Sketch of the ways of adopting the social behavior on interdependent lattices.** (a) connected propagation: At  $t = 1$ , the individual  $A_i$  is successfully exposed to one adopted neighbor, and now the number of new received information is  $m_i(1) = 1$  and  $m_i$  increases by 1. There are no more new adopted neighbors over the next  $k - 2$  time steps, and  $m_i$  remains unchanged. At  $t = k$ , two new adopted neighbors successfully transmit the information to  $i$ , and now  $m_i(k) = 2$ . The individual  $A_i$  becomes adopted with probability  $\pi(m_i)$ , where  $m_i = \sum_{t=0}^{t=k} m_i(t) = 3$ . (b) dependency propagation: At  $t = k$ ,  $A_i$ 's dependency node  $B_i$  becomes adopted immediately due to the dependency propagation.

dependent of the cumulative pieces of information from its adopted neighbors [see Fig. 1(a)]. We designate this type of behavior adoption *connected propagation*. Considering the non-redundant information diffusion in some social contagion processes [34], here we assume that a susceptible individual  $i$  adopts the behavior with probability

$$\pi(m_i) = 1 - (1 - \epsilon)^{m_i}, \quad (1)$$

where  $m_i$  is the susceptible individual's cumulative number of information received from its distinct neighbors, and  $\epsilon$  is the unit adoption probability. A susceptible individual can also adopt the new behavior when its corresponding dependency node in another lattice becomes adopted. We designate this type of behavior adoption *dependency propagation* [see Fig. 1(b)].

The simulations of the social contagion dynamics are implemented as follows. Initially, only 0.05% of individuals are randomly selected to be adopted, and we leave all other individuals in the susceptible state. Each individual has a record  $m_i$  of accumulative numbers of information received from adopted neighbors till now, and  $m_i$  is initially set to 0 for every individual. At each time step, each adopted individual tries to transmit the behavior information to its susceptible neighbors in the same lattice with probability  $\beta$  via

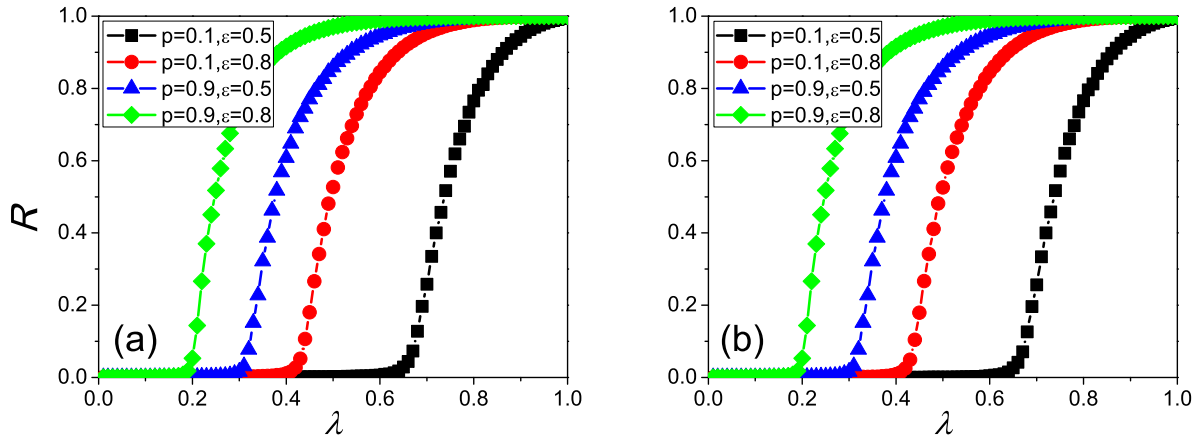


**Figure 2.** (Color online) **The prevalence  $R$  as a function of  $\lambda$  within different parameters in lattice  $A$  (a) and lattice  $B$  (b), respectively.** We perform the experiments on  $10^2$  different networks with  $N = 10^4$ , each of which are tested in  $10^3$  independent realizations.

the connectivity links. If a susceptible node  $i$  is successfully exposed to the information from an adopted neighbor for the first time, its  $m_i$  increases by one and here the adoption probability becomes  $\pi(m_i + 1)$ . Once the node  $i$  becomes an adopted one, its susceptible dependency node becomes adopted immediately because of the dependency infection. At the same time, infected nodes may lose interest in the social behavior and become recovered with a probability  $\mu$ . When an adopted node becomes recovered, it no longer takes part in the propagation of the social behavior. The recovery probability  $\mu$  is set to 1 unless was specific explained. The time step is discrete and increases by  $\Delta t = 1$ . The dynamics of social contagion evolve until there are no more adopted nodes throughout the network.

### 3. Results

In this section, we perform extensive numerical simulations of the interdependent spatial contagion process. The spreading probability  $\lambda$ -dependent of the prevalence (i.e., the average density of final recovered individuals) in lattice  $A$  is analyzed in Fig. 2 (a). In the given network, the large adoption probability could ensure a high information adoption rate and advance the prevalence obviously. Compared with the cases in networks with small  $p$ , the behavior occurs more easily in the networks with large  $p$  due to the effect of abundant dependency infection. Fig. 2 (b) shows the analyses in lattice  $B$ , where the results are almost the same because of the symmetrical characteristic of the social contagions on interdependent lattice networks. Unless otherwise specified, the following analyses will use lattice  $A$  as an example.

In Fig. 3, we further perform the finite-size analysis by computing the the normalized size of first giant connected component (i.e.,  $G^1$ ) for different lattice size  $L$ . In each subgraph, the  $G^1$  curves begin to converge after some  $\lambda$ . For example, the converge point is  $\lambda \approx 0.73$  for  $p = 0.1, \epsilon = 0.5$ . The results show that although the parameters  $p$  and  $\lambda$  have significant

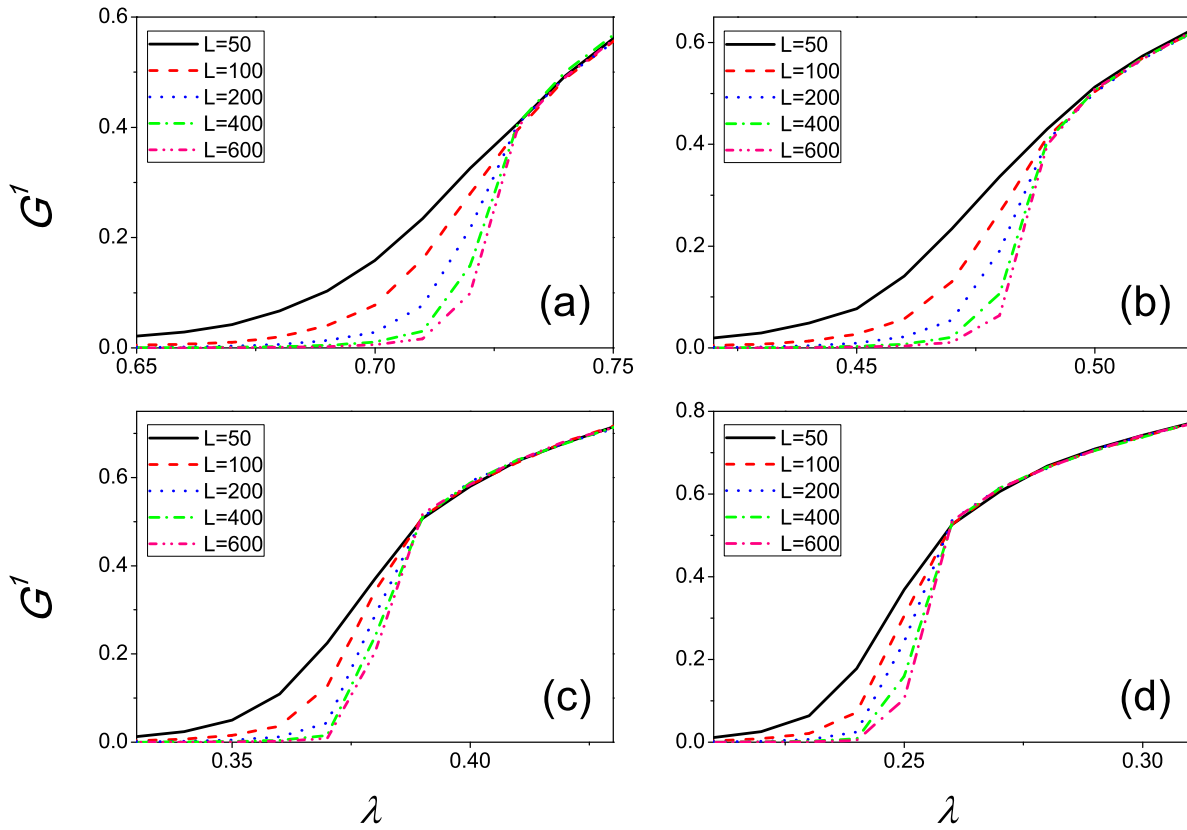


**Figure 3.** (Color online) **The prevalence  $R$  as a function of  $\lambda$  within different  $L$ .** In subfigures (a)-(d), the parameters are respectively chosen as  $p = 0.1, \epsilon = 0.5$ ,  $p = 0.1, \epsilon = 0.8$ ,  $p = 0.9, \epsilon = 0.5$  and  $p = 0.9, \epsilon = 0.8$ . We perform the experiments on  $10^2$  different networks, each of which are tested in  $10^3$  independent realizations.

effects on the prevalence as a function of spreading probability  $\lambda$ , we always observe the second-order phase transition [44].

For the given spreading probability  $\lambda$  and the ratio of dependency node  $p$ , we plots the prevalence as a function of  $\epsilon$  in Fig. 4 (a). For the small  $\lambda$  and  $p$ , both the connected propagation and the dependency propagation are suppressed. Under such circumstances, it's difficult for the social contagion to break out, although the adoption probability is large enough. The large  $\lambda$  improves the success rate of information transmission among neighbors in the same lattice, which stimulates further the adoption of the social behavior, especially in the case of large  $p$ . Moreover, we plot the normalized size of the first largest components (i.e.,  $G^1$ ) for the recovered nodes in Fig. 4 (b). The results again demonstrate that the large spreading probability or strong interdependent networks could obviously promote the social contagion. Remarkably, the  $G^1$  has an abrupt change from the value close to zero to the finite value in the case of  $p = 0.9, \lambda = 0.7$ .

To have a deep understanding of the above phenomena, we perform the finite-size analysis in Fig. 5. The  $G^1$  curves begin to converge after some  $\epsilon$  in Figs. 5 (a) and (b).

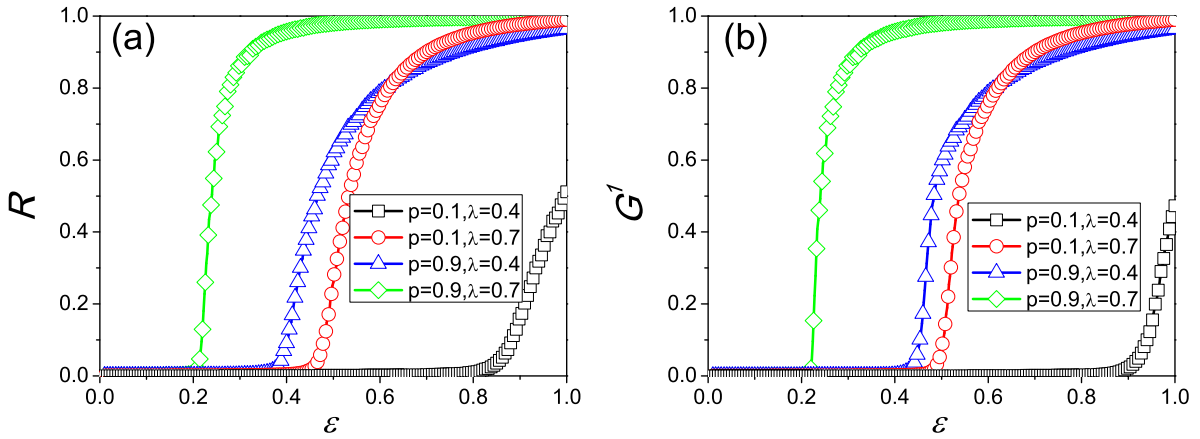


**Figure 4.** (Color online) **Comparison of the prevalence (a) and normalized size of the first largest components for recovered nodes (b) as a function of  $\epsilon$  within different parameters.** We perform the experiments on  $10^2$  different networks with  $N = 10^4$ , each of which are tested in  $10^3$  independent realizations.

In Figs. 5 (c) and (d), we see that all the curves intersect at one point. The intersect points are  $\epsilon \approx 0.476$  and  $\epsilon \approx 0.228$  respectively for  $p = 0.9, \lambda = 0.4$  and  $p = 0.9, \lambda = 0.7$ . These numerical results demonstrate that the parameter  $p$  plays an important role in both the prevalence versus  $\epsilon$  and the spreading form of the social behavior. When  $p$  assumes a relatively large value, even a small fraction of initial spreaders are able to stimulate the propagation in the form of a first-order phase transition, while for a relatively small value, the social behavior spreads in the form of a second-order phase transition [44].

In order to locate the critical point of transition [45, 46] accurately to further support our findings, we use the method developed by Parshani *et al* [47]. For the first-order phase transition, we calculate the number of iterations (i.e., NOI) in the contagion process required for the system to reach a steady state. For the second-order phase transition, we calculate the normalized size of second largest components (i.e.  $G^2$ ) after the contagion process is complete. The two quantities tend to exhibit exceptionally large values at a critical parameter value in the finite network [44]. Fig. 6 shows these as typical of  $p = 0.1, \lambda = 0.4$  and  $p = 0.9, \lambda = 0.7$ . Fig. 6 (a) shows that when  $p = 0.1, \lambda = 0.4$ , the peak of  $G^2$  versus  $\epsilon$  gradually shifts to the right as  $L$  increases. The value of  $\epsilon$  corresponding to the peak for each  $L$  is determined as the critical point  $\epsilon_c^{II}(L)$ . To give the scaling relation near the critical points [48], we fit  $\epsilon_c^{II} - \epsilon_c^{II}(L)$  versus  $1/L$  by using the least-squares-fit method in Fig. 6 (b), and find  $\epsilon_c^{II} - \epsilon_c^{II}(L) \sim (1/L)^{0.5516}$  at  $\epsilon_c^{II} = 0.9875$ . Fig. 6 (c) shows that when  $p = 0.9, \lambda = 0.7$ , the peak of NOI versus  $\epsilon$  gradually shifts to the left with  $L$ . We further fit  $\epsilon_c^I(L) - \epsilon_c^I$  versus  $1/L$  by using the least-squares-fit method in Fig. 6 (d), and find that  $\epsilon_c^I(L) - \epsilon_c^I \sim (1/L)^{0.2089}$  at  $\epsilon_c^I = 0.2089$ . The large second-order transition points and the relatively small first-order transition points explain the variations in prevalence at some extents.

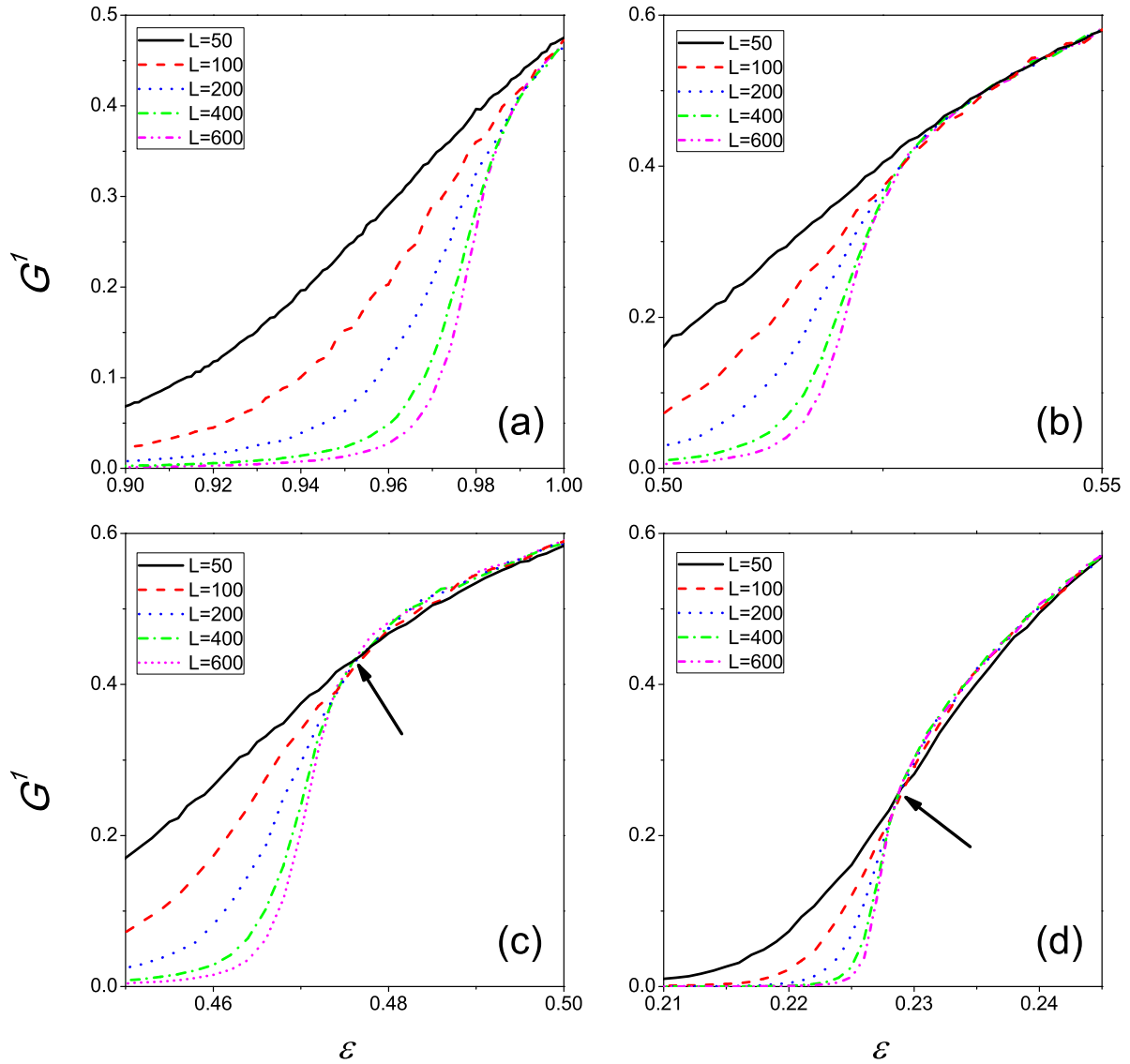


**Figure 5.** (Color online) **The prevalence  $R$  as a function of  $\lambda$  within different  $L$ .** In subfigures (a)-(d), the parameters are respectively chosen as  $p = 0.1, \lambda = 0.4$ ,  $p = 0.1, \lambda = 0.7$ ,  $p = 0.9, \lambda = 0.4$  and  $p = 0.9, \lambda = 0.7$ . The results are averaged over  $10^2 \times 10^3$  independent realizations in  $10^2$  networks.

#### 4. Conclusions

We have studied the complex contagions on interdependent spatial networks consisting of two interdependent lattices. A general threshold model is proposed to describe the individuals' memory effect in the social contagion. In view of this model, a susceptible individual adopts a new behavior with a probability in proportion to the cumulative pieces of information received from its adopted neighbors in the same lattice, or if its dependency node becomes adopted. We first investigated the prevalence versus spreading probability  $\lambda$ . Although the large adoption probability  $\epsilon$  could promote the social contagion significantly in both the weak

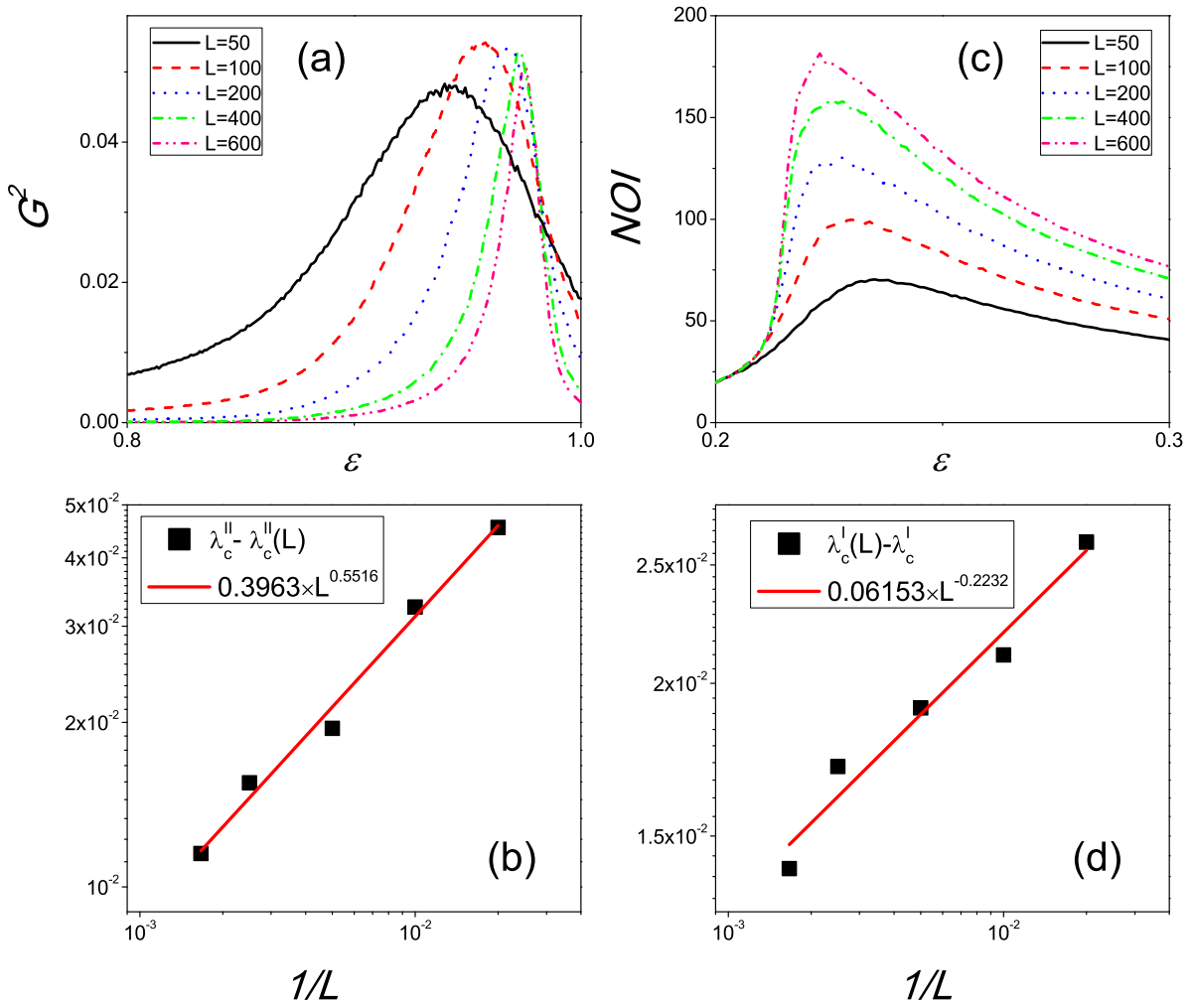


**Figure 6.** (Color online) **The finite-size analyses near the critical points for  $p = 0.1, \lambda = 0.4$  (a-b) and  $p = 0.9, \lambda = 0.7$  (c-d).** (a)  $G^2$  versus  $\epsilon$ . (b)  $\lambda_c^{II} - \lambda_c^{II}(L)$  versus  $1/L$ . (c) NOI versus  $\epsilon$ . (d)  $\lambda_c^I(L) - \lambda_c^I$  versus  $1/L$ . The arrows in (c) and (d) mark the intersection points. The results are averaged over  $10^2 \times 10^3$  independent realizations in  $10^2$  networks.

and strong interdependent networks, the phase transition of prevalence is second-order. For the given spreading probability, we further studied the prevalence versus adoption probability  $\epsilon$ , and found that the strong interdependent structure could obviously stimulate the prevalence. Especially, in the strong interdependent networks we observed the first-order phase transition even for a quite small spreading probability, while the phase transition remains second-order in the weak interdependent networks. Both of the scaling relations near the transition points of first-order and second-order were revealed using the finite-size analysis.

Our results show the important role of the spatial interdependent structure in complex contagions and may help to understand the phase transitions in the social contagion process. Further theoretical studies are very important and full of challenges since the non-Markovian character of our model and non-local-tree like structure of the interdependent lattice make it extremely difficult to describe the strong dynamical correlations among the states of

neighbors.

## Acknowledgements

This work was supported by National Natural Science Foundation of China (Grant No. 61703330).

## References

- [1] Barthélemy M 2011 Phys. Rep. **499** 1
- [2] Li D, Kosmidis K, Bunde A and Havlin S 2011 Nat. Phys. **7** 481
- [3] Boccaletti S, Bianconi G, Criado R, del Genio C I, Gómez-Gardeñes J, Romance M, Sendiña-Nadal I, Wang Z and Zanin M 2014 Phys. Rep. **544** 1
- [4] Balcana D, Colizza V, Gonçalves B, Hu H, Ramasco J J and Vespignani A 2009 Proc. Natl. Acad. Sci. **106** 21484
- [5] Son S W, Grassberger P and Paczuski M 2011 Phys. Rev. Lett. **107** 195702
- [6] Jiang L L and Perc M 2013 Sci. Rep. **3** 02483
- [7] Shekhtman L M, Berezin Y, Danziger M M and Havlin S 2014 Phys. Rev. E **90** 012809
- [8] Wang B, Tanaka G, Suzuki H and Aihara K 2014 Phys. Rev. E **90** 032806
- [9] Morris R G and Barthelemy M 2012 Phys. Rev. Lett. **109** 128703
- [10] Li W, Bashan A, Buldyrev S V, Stanley H E and Havlin S 2012 Phys. Rev. Lett. **108** 228702
- [11] Bashan A, Berezin Y, Buldyrev S V and Havlin S 2013 Nat. Phys. **9** 667
- [12] Zhao J, Li D, Sanhedrai H, Cohen R and Havlin S 2015 Nat. Commun. **7** 10094
- [13] Berezin Y, Bashan A, Danziger M M, Li D and Havlin S 2015 Sci. Rep. **5** 08934
- [14] Kleinberg J M 2000 Nature **406** 845
- [15] Gao J, Zhou T and Hu Y 2015 Sci. Rep. **5** 14662
- [16] Xia C Y, Meng X K and Wang Z 2015 PLoS ONE **10** e0129542
- [17] Li D, Qin P, Wang H, Liu C and Jiang Y 2014 Europhys. Lett. **105** 68004
- [18] Bond R M, Fariss C J, Jones J J, Kramer A D I, Marlow C, Settle J E and Fowler J H 2012 Nature **489** 295
- [19] Wang W, Tang M, Zhang H F and Lai Y C 2015 Phys. Rev. E **92** 012820
- [20] Wang W, Shu P, Zhu Y X, Tang M and Zhang Y C 2015 Chaos **25** 103102
- [21] Wang W, Tang M, Shu P and Wang Z 2016 New J. Phys. **18** 013029
- [22] Ruan Z, Iníguez G, Karsai M and Kertész J 2015 Phys. Rev. Lett. **115** 218702
- [23] Cozzo E, Baños R A, Meloni S and Moreno Y 2013 Phys. Rev. E **88** 050801(R)
- [24] Czaplicka A, Toral R and San Miguel M 2016 Phys. Rev. E **94** 062301
- [25] Rojas F V and Vazquez F 2017 Phys. Rev. E **95** 052315
- [26] Hu Y, Havlin S and Makse H A 2014 Phys. Rev. X **4** 021031
- [27] Gallos L K, Rybski D, Liljeros F, Havlin S and Makse H A 2012 Phys. Rev. X **2** 031014
- [28] Young H P 2011 Proc. Natl. Acad. Sci. USA **108** 21285
- [29] Centola D 2011 Science **334** 1269
- [30] Centola D 2010 Science **329** 1194
- [31] Dodds P S and Watts D J 2004 Phys. Rev. Lett. **92** 218701
- [32] Dodds P S and Watts D J 2005 J. Theor. Biol. **232** 587
- [33] Weiss C H, Poncela-Casasnovas J, Glaser J I, Pah A R, Persell S D, Baker D W, Wunderink R G and Amaral L A N 2014 Phys. Rev. X **4** 041008
- [34] Centola D and Macy M 2007 Am. J. Sociol. **113** 702
- [35] Gao L, Wang W, Shu P, Gao H and Braunstein L A 2017 Europhys. Lett. **118** 18001
- [36] Watts D J 2002 Proc. Natl. Acad. Sci. USA **99** 5766
- [37] Whitney D E 2010 Phys. Rev. E **82** 066110

- [38] Gleeson J P 2008 Phys. Rev. E **77** 046117
- [39] Nematzadeh A, Ferrara E, Flammini A, and Ahn Y Y 2014 Phys. Rev. Lett. **113** 088701
- [40] Lee K M, Brummitt C D and Goh K I 2014 Phys. Rev. E **90** 062816
- [41] Brummitt C D, Lee K M and Goh K I 2012 Phys. Rev. E **85** 045102(R)
- [42] Yağan O and Gligor V 2012 Phys. Rev. E **86** 036103
- [43] Shu P, Gao L, Zhao P, Wang W and Stanley H E 2017 Sci. Rep. **7** 44669
- [44] Liu R R, Wang W X, Lai Y C and Wang B H 2012 Phys. Rev. E **85** 026110
- [45] Boguñá M, Castellano C. and Pastor-Satorras R 2013 Phys. Rev. Lett. **111** 068701
- [46] Shu P, Wang W, Tang M, Zhao P and Zhang Y C 2016 Chaos **26** 063108
- [47] Marro J and Dickman R 1999 *Nonequilibrium Phase Transitions in Lattice Models* (Cambridge: Cambridge University Press)
- [48] Radicchi F and Castellano C 2015 Nat. Commun. **6** 10196